CONNECTING AFRICAN EASTERLY WAVE DEVELOPMENT AND OFFSHORE PRECIPITATION

Patrick Thornton[1], Shun-Nan Wu[2], and Naoko Sakaeda[2]

[1]National Weather Center Research Experiences for Undergraduates Program
Norman, Oklahoma
[2]The School of Meteorology at the University of Oklahoma
Norman, Oklahoma

ABSTRACT

Meridional wind data from radiosondes launched from the island of Sal, Cabo Verde is used to connect African Easterly Wave development and precipitation near coastal West Africa. We utilize the direction of meridional wind to identify the relative position of the waves to Sal. We find that on days with northerly winds, rainfall is enhanced to the south and west, near the inter-tropical convergence zone. On days with southerly winds, precipitation is enhanced in the coastal region and sparse to the southwest. Based on these results, we define two regions, one right on the West African coast, and a second further south and west, towards the Intertropical Convergence Zone to compare the amount of precipitation in these regions with the meridional wind magnitude associated with the AEWs at the Sal Island. We find that there is little relationship between meridional wind strength and precipitation amounts, although there is a slight tendency for more coastal precipitation when southerly winds are stronger on Sal, and more Intertropical Convergence Zone precipitation when northerly winds are stronger on Sal. These findings emphasize the importance of the location of AEWs when forecasting, especially considering how precipitation distribution is dependent on it.

1. INTRODUCTION

African Easterly Waves (AEWs) are the dominant synoptic-scale system that exerts significant control over rainfall variability in the tropical North Atlantic and the adjacent coastal regions. The associated extreme rainfall events frequently lead to detrimental social and economic consequences in the populated area over Atlantic coastal regions and Caribbean islands. A better understanding of how AEWs evolve during their critical development period can advance the prediction skills for these extreme rainfall events. This study aims to investigate the structure of AEWs and their corresponding precipitation over coastal West Africa to advance the understanding of AEW transition from land to ocean.

AEWs are synoptic-scale waves that initiate in northern Africa and propagate westward, having wavelengths spanning up to 4000 km (Kiladis et al. 2006). The wind speed of AEWs has a peak occurring close to the level of the African Easterly Jet (AEJ) at around 700 hPa. Near the surface, northerly winds maximize ahead of AEW troughs, and southerly winds maximize behind them (Kiladis et al. 2006). As the waves propagate westward over Africa, they eventually reach the transitional coastal region, offshore to the Atlantic Ocean, and potentially develop into tropical cyclones (Reed et al. 1977).

During summer in the northern hemisphere, AEWs dominate rainfall variability in tropical West Africa (Kiladis et al. 2006). These extreme rainfall events are mainly contributed by the Mesoscale Convective Systems (MCSs) associated with AEWs (Payne and McGarry 1977; Machado et al. 1993). Over land, these MCSs appear ahead, or to the west, of the AEW troughs, whereas over the ocean, the MCSs appear behind, or to the east, of these troughs (Kiladis et al. 2006). North of the AEJ axis, the convective region is consistently behind the trough (Kiladis et al. 2006). However, these associated convective activities over coastal West Africa, as the waves transition from a continental environment to a marine one, remain unclear. In addition, the climatological rainfall maximum occurs offshore within this coastal region (Hamilton et al. 2016), urging a better understanding of the role of AEW passage in contributing to the rainfall in the coastal region.

Variability in AEW structure in this coastal region is high; two consecutive waves may have different precipitation distribution and rates. Therefore, in-situ observations near coastal West Africa have been insufficient to further investigate the relationship between AEWs and their associated precipitation over this coastal transition region. To address this, NASA's Convective Processes Experiment - Cabo Verde (CPEX-CV) field campaign was conducted during September 2022 on the island of Sal, Cabo Verde, which is about 450 miles west of the African coastline, and collected a month of radiosonde data on the island. This project aims to utilize in-situ observations obtained from NASA CPEX-CV to clarify the relationship between AEW activity and its associated precipitation over the coastal region.

In this study, we investigate two primary relationships: one being the relationship of the positioning and timing of AEWs observed on Sal to the precipitation distribution over the coastal region, and the other being the relationship between the strength of a wave and the amount of associated offshore precipitation. Firstly, we propose that a relative maximum in offshore rainfall rates occurs approximately one day prior to the arrival of an AEW to Sal due to enhanced onshore convergence from the AEW flow. Secondly, we propose that more intense AEWs would cause greater coastal rainfall amounts as a result of enhanced onshore convergence.

2. DATA AND METHODS

The primary data used in this project is radiosonde data from Sal collected during CPEX-CV. This was a field campaign designed to be a continuation of 2021's cut short Convective Processes Experiment - Aerosols and Winds (CPEX-AW). Based on the island of Sal, Cabo Verde, the campaign's goals were to study convection in the eastern tropical Atlantic, as well as to gather more data on the Saharan Air Layer and fill in other gaps in observational data. Radiosondes were launched at least twice daily in the morning and evening with mostly regular intervals, and third radiosondes were often launched midday. In total, 75 radiosondes were launched. Flights also went out to gather more

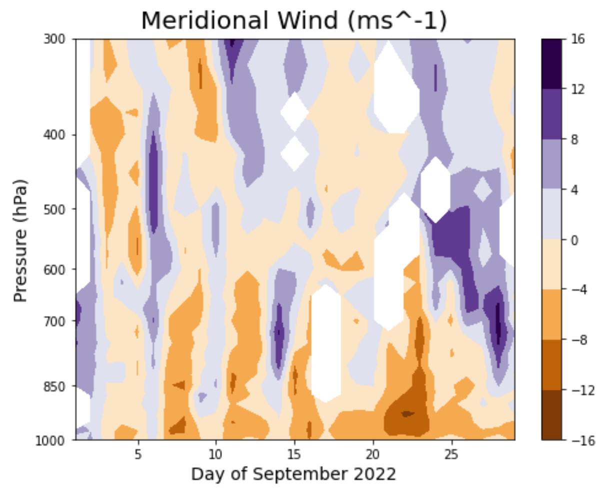

FIG 1. Plot depicting meridional wind from 1000 to 300 hPa from radiosonde data from the island of Sal, Cabo Verde, during the month of September 2022

data in the coastal region utilizing dropsondes, but these data were not used in this project.

The launched radiosondes measured high-resolution vertical profiles of atmospheric properties, including pressure, temperature, dew point, meridional wind, zonal wind, relative humidity, and others. Most data were properly gathered and quality controlled, except for a few issues that occurred for specific variables for certain times, which are excluded for this research. At least two radiosondes were launched every day from September 2nd to September 29th, except for September 1st, 2022, which had only one radiosonde launch. Because launches were not exactly consistent with timings and some days had more than others, we computed the daily average of data to represent associated AEW activity for each day. In order to better understand and visualize the radiosonde data, we interpolated data to pressure intervals of 25 hPa from 1000 hPa to 300 hPa. Figure 1 displays the meridional wind data throughout the month from 1000 hPa to 300hPa, with negative values depicting northerlies, and positive values depicting southerlies.

We also use Integrated Multi-satellitE Retrievals for GPM (IMERG) data, which is an algorithm that uses the GPM satellite constellation to estimate global precipitation data, with a spatial resolution of 0.1° by 0.1° and a 30 minute temporal interval (Huffman et al. 2015). We use the IMERG data set to examine rainfall rates in the coastal region.

For investigating the relationship between AEW position and offshore rainfall maximum

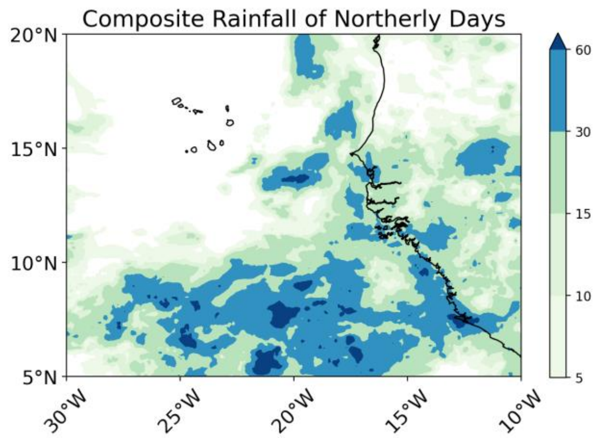

FIG 2. The composite of daily accumulated rainfall over coastal West Africa for northerly wind days on Sal, Cabo Verde. Shadings are daily accumulated rainfall in mm. Horizontal and vertical axes are longitude and latitude in degrees, respectively.

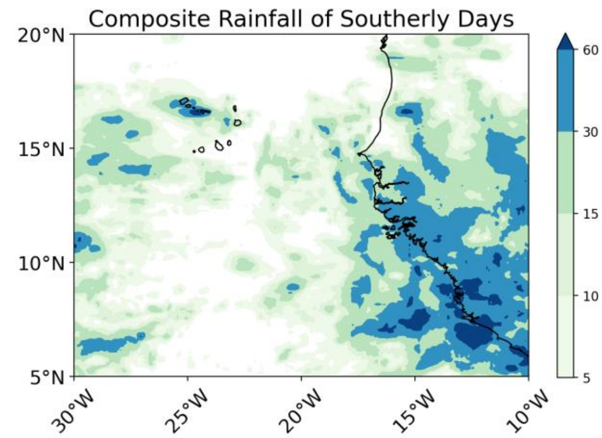

FIG 3. Same as Figure 2, but for southerly wind days on Sal

location, we create the composites of precipitation as a function of three categories of meridional wind direction and transition: northerlies above half of one standard deviation from the mean, southerlies above half of one standard deviation from the mean, and days without significant northerlies or southerlies. Overall, the mean meridional wind is -1.599 m/s, and the standard deviation is 3.94 m/s. These wind values are calculated by averaging the meridional wind from 1000 to 600 hPa. Days where the meridional wind exhibits these characteristics are put into these categories. With this, we could determine the relative location of a passing AEW. During days with northerlies, an AEW trough is heading towards Sal, and when southerlies are dominant, the AEW trough exits west of Sal. On days where there are neither significant northerlies nor southerlies, Sal is either right below the trough, or in between waves. In total, there are seven days with southerly flow, nine days with northerly flow, and thirteen days with neither. By comparing composite images of the IMERG data for the dates of each category, we can determine which category corresponds to the highest coastal rainfall rates.

For testing how AEW intensity affects offshore precipitation amounts, we compare the strength of AEWs through meridional wind speed with the associated offshore precipitation. For meridional wind speed, we used northerlies, as that was when the wave was still approaching the island. Then, we compared the strength of the AEWs' meridional wind speeds and the amount of precipitation indicated through IMERG data in two designated regions: a coastal region, bounded by 18°-11°W and 5°-14°N, and an Intertropical Convergence Zone (ITCZ) region, bounded by 28°-15°W and 5°-10°N.

3. Results

The following will consist of the primary results from both the precipitation and AEW location relationship and the precipitation and AEW strength relationship. First, figure 2 displays the composite rainfall averaged over all nine days with significant northerly winds at Sal from 10°-30°W and 5°-20°N, derived from the IMERG data, in mm/day. Rainfall is highest in the south, between 5°-10°N, but still prevalent north and east, along the African coastline past 15°N. Comparatively, rainfall near the Cabo Verde islands and Sal itself is sparse to non-existent.

When these northerly winds occur at Sal, the longitude of the AEW trough axis is typically near the center of the region of higher rainfall. Thus, it is likely that the rainfall is a result of moisture advected northwards by the AEW trough. The area to the west and near Cabo Verde is typically on the leading edge or further ahead of an approaching AEW trough, where the flow would be advecting dry Saharan air into the region. This is a likely explanation for the lack of precipitation near Cabo Verde on these northerly days.

Figure 3 displays the same as Figure 2, but shows the composite rainfall averaged over the seven days with significant southerly wind at Sal. In comparison to days with northerly wind, there is far less precipitation further south towards

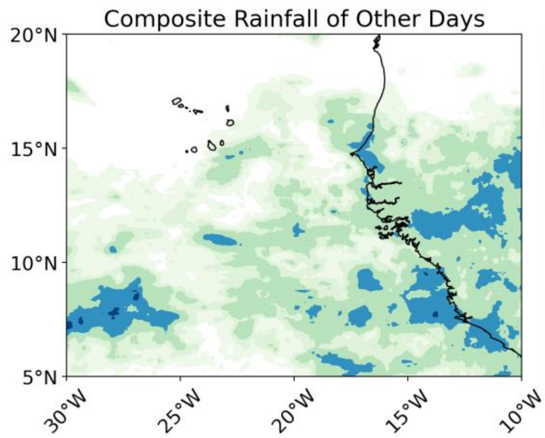

FIG 4. Same as Figure 2 and 3, but for days with neither northerly nor southerly wind on Sal

the ITCZ, and conversely, there is more precipitation along the coastline. Rainfall is not entirely absent near the ITCZ, and is now present near Cabo Verde, unlike during northerly days.

Because southerly winds at Sal are associated with AEW troughs to the west of Cabo Verde, it is highly probable that the high coastal precipitation is unassociated with the AEW causing the southerly winds and is instead associated with the succeeding AEW. In this case, Cabo Verde is on the east edge of the AEW trough, and the southerly winds at Sal would be advecting moisture northward, explaining the presence of precipitation in and around Cabo Verde.

Figure 4, like the two previous figures, shows composite rainfall, but for days considered to have neither significant northerlies nor southerlies. Here, rainfall is spread relatively evenly when compared to northerly and southerly days. Moderate precipitation occurs both along the coast, and close to the ITCZ. Light precipitation occurs near Cabo Verde as well.

As meridional wind was not significant in either direction, these results show that precipitation is more widespread when the AEW trough axis is at the same longitude as Sal, or Sal is directly in between AEWs. However, with this methodology, we cannot differentiate whether Sal is between AEWs or in the center of one, but as areas between two AEWs troughs are typically much drier (Gu et al. 2004), the majority of rainfall on days with neither clear wind direction likely occurs when Sal is in the center of the AEW trough, but further investigation on this topic may be beneficial.

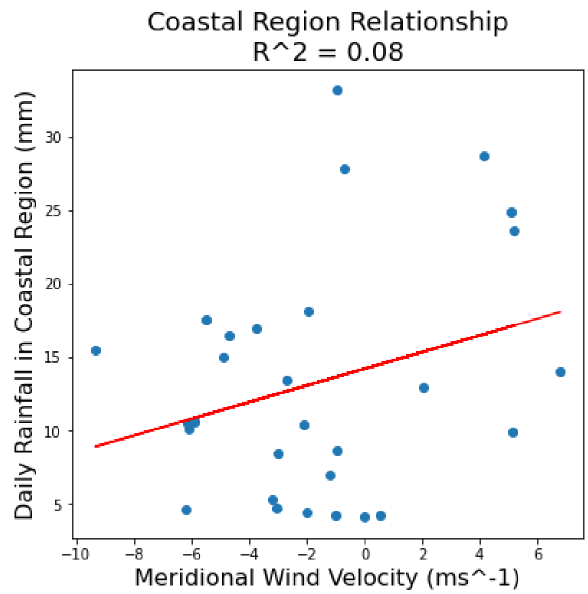

FIG 5. Scatterplot depicting the relationship between daily precipitation in the coastal region and meridional wind velocity on Sal. Horizontal and vertical axes are meridional wind velocity in m/s and daily rainfall in the coastal region in mm, respectively.

This segment of results indicates that coastal rainfall is most enhanced when southerly winds occur at Sal, and rain near the ITCZ is most enhanced when northerly winds occur at Sal. This contradicts the hypothesis that coastal rainfall is maximized about one day before an AEW arrival, as that would coincide with northerly winds, rather than the southerly winds results indicate. Furthermore, this indicates the importance of forecasting timing and location of AEWs, as precipitation location is dependent on the location of AEWs. If forecasts are better able to predict AEW location, precipitation forecasts could become more accurate as a result.

Continuing, Figure 5 is a scatterplot showing the relationship between daily rainfall in the coastal region defined in the methods section in mm, and the meridional wind velocity from the radiosondes launched from Sal in m/s. Each blue dot represents a single day, with 29 days total representing September 1st through September 29th, 2022. The red line is the line of best fit, which attempts to show a linear relationship between the daily rainfall in the coastal region and the meridional wind. As seen by the distance between dots and the line of best fit, the linear association between the two is tenuous, but the tendency indicates more coastal rainfall with southerly winds.

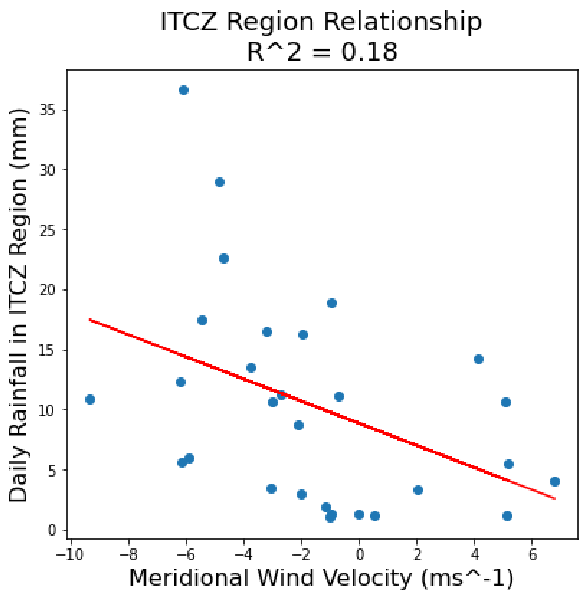

FIG 6. Same as Figure 5, but for the ITCZ region instead of the coastal region

The relationship in the coastal region only had a coefficient of determination (R^2) of 0.08, which signifies that there is very little linearity between the meridional wind at Sal and coastal precipitation totals. However, this should be expected. The AEW causing the southerly wind at Sal is most likely not associated with the coastal precipitation, but the next AEW, still over Africa, likely is. For this to be investigated further, analysis of wind should be gathered from continental Africa rather than from Cabo Verde. Even so, the slight tendency for the precipitation to be higher as winds are more southerly lines up with the previous results that coastal precipitation is higher when southerly winds occur at Sal.

Finally, Figure 6 is another scatterplot, however, this time it shows the relationship between daily rainfall in the defined ITCZ region and meridional wind velocity. Here, the linear association is clearer, but still not very strong. In this case, the tendency indicates more rainfall in the ITCZ region when northerly winds occur at Sal.

The ITCZ region has a slightly higher R^2 of 0.18, which still shows that there is little linear relationship between ITCZ rainfall totals and meridional wind at Sal, however it is stronger than the relationship in the coastal region. The rainfall in the ITCZ region appears to be linked to the AEW causing the northerly winds at Sal, unlike the rainfall in the coastal region, which could provide an explanation for that stronger relationship. Once again, the modest tendency that is exhibited lines up with previous results, as precipitation in the ITCZ region tends to be higher during days with northerly winds.

Ultimately, this result did not indicate a strong relationship between AEW strength and precipitation amounts. While it did display a tendency which aligns with the other results, the linear relationship was too weak to be conclusive. Further research should be done in this area by using other proxies for AEW strength like vorticity magnitude to see if there is a stronger relationship with precipitation amounts.

4. SUMMARY AND CONCLUSIONS

Analysis of radiosonde data obtained from the island of Sal, Cabo Verde, along with IMERG precipitation data leads us to conclude that there is a connection between meridional wind direction and precipitation location. When northerly winds are present at Sal, precipitation is enhanced near the ITCZ region southwest of the West African coast, and when southerly winds are present at Sal, precipitation is enhanced just along the coastline of West Africa. Meridional wind velocity and precipitation amounts have a low correlation coefficient in defined coastal and ITCZ regions, but the coastal region tends to have higher precipitation when winds are southerly at Sal, and the ITCZ region tends to have higher precipitation when winds are northerly at Sal.

It should be noted that this study only uses radiosonde data from a single location on Sal, and thus all work is tied to that location and directly surrounding regions. The single data location limits a broader range of investigation. For example, coastal precipitation was maximized before the associated AEW even affected Sal. However, there is a wealth of data that can be utilized from the radiosondes alone, and more analysis can be done using other variables, like humidity and temperature.

These results show that there is value in utilizing observational data from Cabo Verde in looking at the greater structure of passing AEWs. Wind direction alone can assist in diagnosing where precipitation is likely to be ongoing. Forecasts with this in mind can better predict coastal and offshore precipitation based on the timing of AEWs. Furthermore, they also provide a basis to gauge model or simulated data accuracy, or other indirect observations.

5. ACKNOWLEDGEMENTS

This material is based upon work supported by the National Science Foundation under Grant No. AGS-2050267. I would also like to thank Dr. Daphne LaDue and Alex Marmo, co-directors of the Research Experience for Undergraduates program at the National Weather Center for organizing and managing the program, letting this all be possible.

6. REFERENCES

Gu, G., R. F. Adler, G. J. Huffman, and S. Curtis, 2004: African easterly waves and their association with precipitation. *J. Geophys. Res.*, **109** **.**D04101, https://doi.org/10.1029/2003JD003967.

Hamilton, H. L., G. S. Young, J. L. Evans, J. D. Fuentes, and K. M. Núñez Ocasio, 2017: The relationship between the Guinea Highlands and the West African offshore rainfall maximum. *Geophys. Res. Lett.*, **44**, 1158–1166, https://doi.org/10.1002/2016GL071170.

Huffman, G., D. Bolvin, D. Braithwaite, K. Hsu, R. Joyce, P. Xie, 2014: Integrated Multi-satellitE Retrievals for GPM (IMERG), version 4.4. NASA's Precipitation Processing Center, accessed 09 June, 2023, ftp://arthurhou.pps.eosdis.nasa.gov/gpmdata/

Kiladis, G. N., C. D. Thorncroft, and N. M. J. Hall, 2006: Three-Dimensional Structure and Dynamics of African Easterly Waves. Part I: Observations. *J. Atmos. Sci.*, **63**, 2212–2230, https://doi.org/10.1175/JAS3741.1.

Machado, L. A. T., J. Duvel, and M. Desbois, 1993: Diurnal Variations and Modulation by Easterly Waves of the Size Distribution of Convective Cloud Clusters over West Africa and the Atlantic Ocean. *Mon. Wea. Rev.*, **121**, 37–49, https://doi.org/10.1175/1520-0493(1993)121<0037:DVAMBE>2.0.CO;2.

Payne, S. W., and M. M. McGarry, 1977: The Relationship of Satellite Inferred Convective Activity to Easterly Waves Over West Africa and the Adjacent Ocean During Phase III of GATE. *Mon. Wea. Rev.*, **105**, 413–420, https://doi.org/10.1175/1520-0493(1977)105<0413:TROSIC>2.0.CO;2.

Reed, R. J., D. C. Norquist, and E. E. Recker, 1977: The Structure and Properties of African Wave Disturbances as Observed During Phase III of GATE. *Mon. Wea. Rev.*, **105**, 317–333, https://doi.org/10.1175/1520-0493(1977)105<0317:TSAPOA>2.0.CO;2.